doi:10.1016/j.jmb.2005.10.080 J. Mol. Biol. (2006) 355, 640–650

JMB

Available online at www.sciencedirect.com

SCIENCE DIRECT®

ELSEVIER

Characterizing Molecular Interactions in Different Bacteriorhodopsin Assemblies by Single-molecule Force Spectroscopy

K. Tanuj Sapra[1,2], Hüseyin Besir[3], Dieter Oesterhelt[3] and Daniel J. Muller[2]*

[1]*Max Planck Institute of Molecular Cell Biology and Genetics, 01307 Dresden Germany*

[2]*Center for Biotechnology University of Technology 01307 Dresden, Germany*

[3]*Max Planck Institute of Biochemistry, 82152 Martinsried, Germany*

**Corresponding author*

Using single-molecule force spectroscopy we characterized inter- and intramolecular interactions stabilizing structural segments of individual bacteriorhodopsin (BR) molecules assembled into trimers and dimers, and monomers. While the assembly of BR did not vary the location of these structural segments, their intrinsic stability could change up to 70% increasing from monomer to dimer to trimer. Since each stable structural segment established one unfolding barrier, we conclude that the locations of unfolding barriers were determined by intramolecular interactions but that their strengths were strongly influenced by intermolecular interactions. Subtracting the unfolding forces of the BR trimer from that of monomer allowed us to calculate the contribution of inter- and intramolecular interactions to the membrane protein stabilization. Statistical analyses showed that the unfolding pathways of differently assembled BR molecules did not differ in their appearance but in their population. This suggests that in our experiments the membrane protein assembly does not necessarily change the location of unfolding barriers within the protein, but certainly their strengths, and thus alters the probability of a protein to choose certain unfolding pathways.

Keywords: atomic force microscopy; membrane protein assembly; single-molecule force spectroscopy; membrane protein oligomerization; membrane protein stability

Introduction

Membrane proteins carry out a plethora of functions like photosynthesis, transport of ions and small molecules, maintenance of osmotic balance, cell–cell adhesion, and signal transduction. An intriguing and challenging problem is to understand how membrane proteins assemble and form thermodynamically stable structures *in vivo*.[1–4] It is known that intramolecular interactions drive protein folding and most probably contribute, more than intermolecular interactions, in maintaining the functional and structural integrity of the protein.[2] Hence, it is important to explore the nature of intra- and intermolecular interactions not only to understand how these proteins have evolved to form structurally stable, elegant architectures and efficient functional machines,[5] but also to increase our knowledge of how proteins are driven into misfolded conformations in disease states.[6–8]

Bacteriorhodopsin (BR), a seven transmembrane α-helical protein[9] from the archaebacterium *Halobacterium salinarum* is one of the most extensively studied membrane proteins.[10–12] Its structural similarity to the guanine-nucleotide protein coupled receptors (GPCRs),[13–15] the elucidation and availability of various refined structural models[16–19] has made BR a very good model system for biophysical and biological characterization.

In native conditions, BR assembles into trimers that are arranged as a two-dimensional (2D) hexagonal lattice.[20] Recrystallization of BR in the presence of *n*-dodecyl trimethylammonium chloride (DTAC) has been shown to yield well-ordered 2D crystals establishing $p22_12_1$ symmetry. BR in this new crystal form exists as dimers and is

Abbreviations used: BR, bacteriorhodopsin; AFM, atomic force microscopy; WLC, worm-like chain; aa, amino acid.

E-mail address of the corresponding author: mueller@biotec.tu-dresden.de

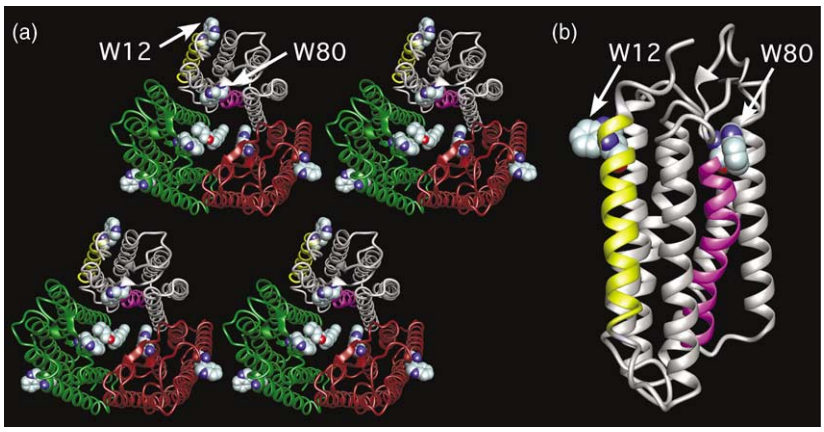

Figure 1. Crystal structure of the BR trimer indicating the mutations inserted at positions W12I and W80I. (a) To emphasize the positions of the mutations at the interfaces of trimeric BR we have displayed the BR in its trigonal lattice (PDB 1BRR).[16] However, the mutant BR was not able to form a crystalline lattice nor did we observe the formation of BR trimers as shown in Figure 2(c). (b) Side-view of the BR monomer showing the mutations W12I and W80I in helices A and C, respectively.

arranged in an orthorhombic lattice.[21] Substitution of tryptophan residues at amino acid positions 12 and 80 with isoleucine residues leads to the collapse of the 2D assembly of BR and most probably to the formation of single monomers. The mutation at amino acid position 12 alters trimer–trimer interactions, and the one at position 80 monomer–monomer interactions within the trimer (Figure 1).[22] The effects of changes in the BR assembly and membrane lipid content on the structural stability of BR have been investigated until now by conventional kinetic and equilibrium methods[23,24] and by neutron diffraction,[22] which are indirect and give an average of the ensemble measurements.

The mechanical unfolding of individual proteins by single-molecule force spectroscopy complements more classical methods using either temperature or chemicals as denaturants.[25,26] Mechanical unfolding experiments performed on single membrane proteins such as BR have revealed that single helices, polypeptide loops and certain structural regions of helices could establish sufficiently strong molecular interactions to form independently stable units.[27–30] Such stable structural segments, which can be represented by grouped, single or parts of secondary structure elements, build unfolding barriers and stabilize the whole membrane protein.

The nature of molecular interactions that establish such stable structural segments within a membrane protein is not well understood though important questions remain to be answered. Are the locations and stability of these structural segments the result of intermolecular (monomer–monomer or oligomer–oligomer), or intramolecular interactions (within the secondary structure elements) or both? How does the protein assembly exhibit an effect on the unfolding forces and pathways? Does it influence the dimensions and positions of the structural segments that form the unfolding barriers? Does altering protein–protein and protein–lipid interactions change the unfolding pathways? To obtain insights into these questions, we unfolded trimeric, dimeric and monomeric BR assemblies using a combination of atomic force microscopy (AFM) imaging and single-molecule force spectroscopy.[27] It was observed that independent of their assembly into different oligomeric states, the lengths and positions of the polypeptide chains that established the unfolding barriers within the BR molecule did not change. However, the mechanical stability of the structural segments and hence the strength of molecular interactions establishing the unfolding barriers depended on the BR assembly.

Results

High-resolution AFM imaging of different BR assemblies

Before performing single-molecule force spectroscopy, the samples were observed at high resolution using AFM in buffer solution (Figure 2). Surveys showed the membranes adsorbed flat onto the supporting mica (Figure 2, top row). On average, the membrane proteins protruded 5.9($\pm$ 0.4) nm from the supporting surface.[31] If recorded at high resolution, the topographs revealed details of different BR assemblies. While BR of purple membrane was arranged into trimers (Figure 2(a)), the dimers assembled into an orthorhombic lattice (Figure 2(b)).[32] Overview topographs of the mutant proteins (Figure 2(c)) suggested that less than 20% of the lipid membrane area (height $\approx$4.1($\pm$0.4) nm) was occupied with membrane proteins (height $\approx$5.7($\pm$0.4) nm). This lower packing density of the membrane could be confirmed by sucrose gradient experiments (data not shown). Additionally, the membranes containing the BR double mutant (W12/80I) showed no apparent crystalline structure (Figure 2(c), bottom). Instead, loosely packed assemblies were observed. High-resolution topographs have not revealed single BR trimers such as those observed previously for bacteriopsin.[33] Individual objects in these protein assemblies had dimensions of single BR molecules and, since the membrane contained only BR, these objects were assumed to be monomeric BR. It was,

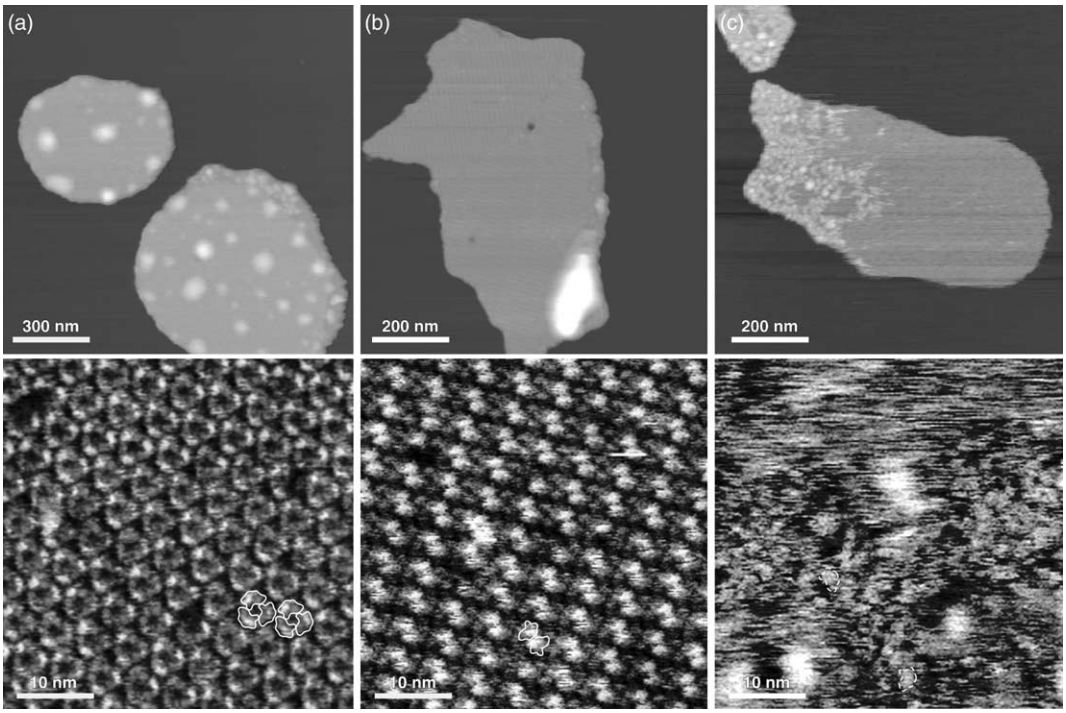

Figure 2. High-resolution AFM topographs of membranes. BR molecules assembled into (a) trimers, (b) dimers, and (c) monomers. Top row, surveys show the membranes being adsorbed flat on mica. The membranes exhibited heights between 5.5($\pm$0.6) nm and 6.4($\pm$0.5) nm. Bottom row, membrane surfaces imaged at high resolution. (a) Trimeric, and (b) dimeric assemblies of BR were clearly resolved. Being distributed at a lower concentration in the membrane as compared to the crystalline BR assemblies, monomeric BR (c) could not be resolved as single particles. Monomers in the lipid bilayer exhibited a higher mobility and could not be imaged at subnanometer resolution as revealed on imaging the crystalline assembly of (a) trimers and (b) dimers. The outlined BR shapes shown in the high-resolution topographs (bottom) represent 0.1 nm thick slices of the cytoplasmic BR surface (Müller *et al.* [32]). In (c) the broken outlines show possible arrangements of single BR monomers. Topographs are displayed in full gray scale corresponding to vertical heights of 20 nm (top row) and 1.2 nm (bottom row).

however, difficult to observe sub-structural details of these BR monomers that had an enhanced mobility due to the reduced BR packing density. In this case, single BR molecules could diffuse freely through the membrane.[34] Compared to this, BR that was densely packed into a 2D crystal lattice exhibited no lateral mobility.

Unfolding pathways of single BR molecules

A schematic interpretation of a typical force–extension curve exhibiting common features observed among all curves is shown in Figure 3(a). The spectrum shows the unfolding pattern of a single BR molecule from a dimeric assembly.[28–30,35] After attachment of the C-terminal end of a BR molecule to the AFM stylus and subsequent separation of the stylus from the purple membrane (PM) surface, the polypeptide end was extended. Further separation of the stylus and membrane stretched the C-terminal end leading to force build-up in a gradual non-linear manner. At a certain threshold force, the first transmembrane helices G and F establishing an unfolding barrier unfolded. This unfolding event, however, in most cases is masked by non-specific interactions occurring at stylus–sample separations smaller than 20 nm.[27,28] Such non-specific interactions contributing to the force–extension curve were scattered, which is highlighted by the superimposition of numerous curves (Figure 3 (c)–(e)). However, the unfolding event of helices G and F increased the length of the unfolded polymer forming the molecular bridge between stylus and membrane. This caused the cantilever to relax as the force dropped abruptly (shown by black arrows). Further separating the AFM stylus and membrane surface extended the polypeptide chain of the unfolded structural elements. As soon as the polypeptide was stretched again the force increased, as detected by the cantilever deflection. At a certain critical force, the next secondary structure element (in terms of the polypeptide chain) that established an unfolding barrier unfolded. The force–extension traces defined by stretching and unfolding of helices could be well fitted using the worm-like chain (WLC) model with only one free parameter: the contour length of the stretched polypeptide segment of the molecule.[25] This fit describes the stretching of an already unfolded part of the protein, marking the end of the preceding and the starting point of the subsequent stable structural element that

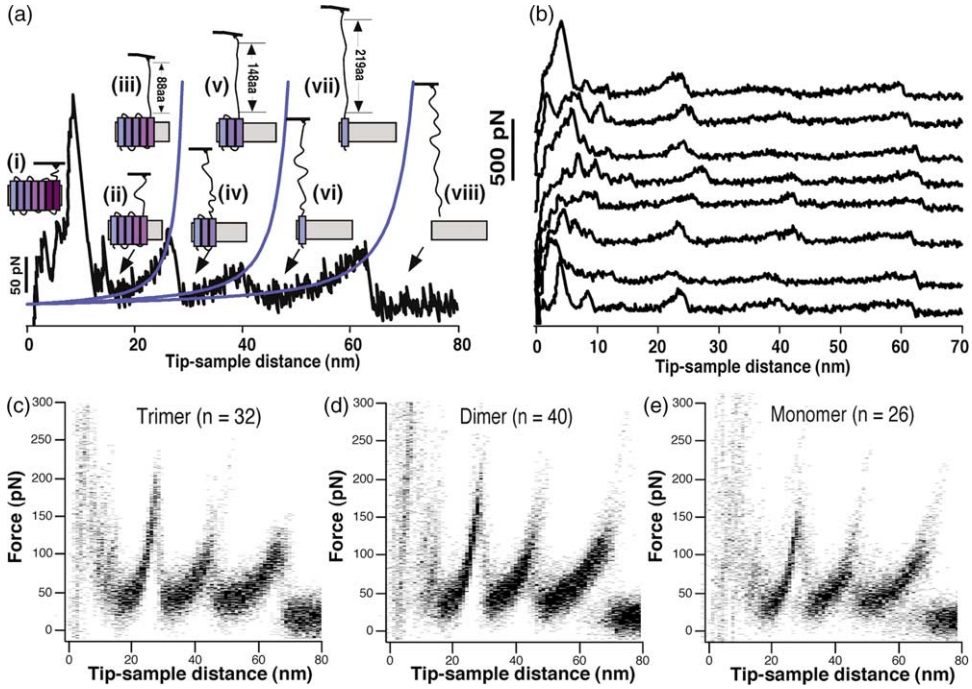

Figure 3. Unfolding pathways of BR trimer, dimer and monomer. (a) Pairwise unfolding pathway of transmembrane α-helices. The spectrum shows a representative unfolding pathway of a single BR dimer molecule.[27–30] The drawings show the unfolding pathways at different positions as unfolding proceeds. Initially the cantilever is brought into contact with the molecule in the native state with a minimum contact force (i). The first force peaks detected within a separation of 0–15 nm to the PM surface indicate the unfolding of transmembrane α-helices F and G, and of loops FG and EF. The peaks within this region are hidden due to non-specific surface interactions between PM and the AFM stylus. After the unfolding event (ii), the number of amino acid residues (aa) stretched is increased to 88 and the cantilever relaxes. Further separating stylus and sample stretches the polypeptide (iii), thereby pulling on helix E. At a certain pulling force, the mechanical stability of helices E and D is insufficient and they unfold together with loops DE and CD (iv). The unfolded helices E and D are now stretched to a length of 148 aa (v), the polypeptide being pulled on helix C. Helices B and C and loops BC and AB unfold in a single step, thereby relaxing the cantilever (vi). By further separating stylus and PM, the cantilever pulls on helix A (vii) until the polypeptide is completely extracted from the membrane (viii). Blue curves represent WLC fits to individual force peaks. (b) Individual force spectrum recorded on single BR dimer molecules. To show the common unfolding patterns among single-molecule events, the force spectra recorded for different BRs were superimposed. Superimpositions show a common unfolding pattern for (c) trimeric BR, (d) dimeric BR, and (e) monomeric BR. The width (spread) of the single peaks is determined by the experimental noise and by standard deviations of these peaks from their average values (Figure 4 and Table 1). Note that the superimpositions only show a fraction of the force-curves that were analyzed statistically ($n > 360$; Table 1 and Figures 4–6).

establishes an intrinsic mechanical unfolding barrier. As shown previously, the fitted contour length of the force–extension curve and the secondary structure model of BR suggest that helices G and F, D and E, and B and C unfolded predominantly in a pairwise manner.[27,28] The remaining seventh helix A was then pulled from the membrane in a single step. Beyond an extension of 70 nm no interaction was measured.

Recently dynamic force spectroscopy (DFS) experiments on single BR molecules allowed the determination of the energy landscape of single structural segments establishing a barrier against unfolding.[29] Individual energy barriers, which had to be crossed to unfold a single transmembrane α-helix or a pair of helices, exhibited widths ranging from 0.3 nm to 0.9 nm. Such small extensions of the structural segments were sufficient to induce their spontaneous unfolding within BR. These results build a strong argument for the assumption that structural segments unfold and leave their embedding membrane.

Unfolding pathways do not depend on BR assembly

Figure 3(c)–(e) shows superimpositions of typical force–extension traces obtained on unfolding single BR molecules. Superimposition of unfolding traces highlights the common unfolding pattern through the accumulation of measured data points (densely plotted areas) and at the same time conserves the individualism of single unfolding events (less densely plotted areas). All force–extension traces of single molecules from trimeric (Figure 3(c)), dimeric (Figure 3(d)) and monomeric (Figure 3(e)) BR assemblies showed three main peaks at amino acid positions 88 (helices E and D), 148 (helices B and C) and 220 (helix A). These main peaks occurred with a probability of 100%.[27–29] In those cases in which the main peak occurred without side peaks they reflected the pairwise unfolding of helices and their connecting loops. Apart from the main unfolding peaks, force–extension curves of all

BR assemblies could exhibit side peaks at polypeptide lengths of 94, 105, 158, 175 and 232 amino acids (Figure 4). Side peaks occurred with lower probabilities, ranging between 10% and 60%. Cases where both main peak and side peaks occurred simultaneously are attributed to the stepwise unfolding of single helices, the connecting loops or of fragments thereof.[28,35] Thus, the secondary

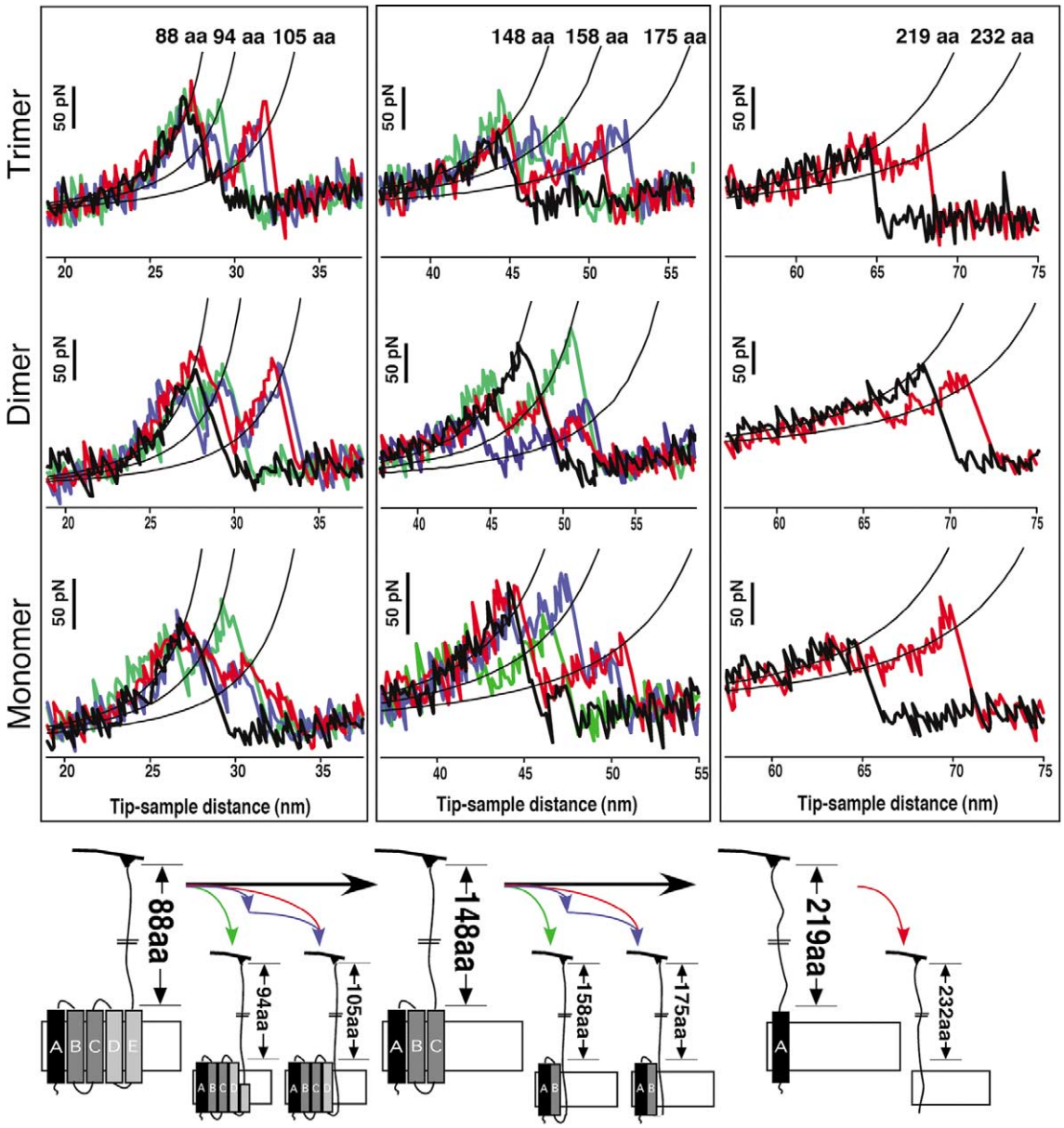

Figure 4. Similar unfolding pathways of trimeric, dimeric and monomeric BR. Unfolding events of individual secondary structure elements; each horizontal row shows the pathways for trimer, dimer and monomer. Black smooth curves represent WLC fits of force peaks used to determine the number of stretched amino acids (aa). WLC fits given are representative for the average of all peaks. Single peaks deviate from these values within the standard deviation (SD) (Table 1). Occasionally, the first unfolding peak at 88 aa shows two shoulder peaks (first column), indicating the stepwise unfolding of the helical pair. If both shoulders occur, the peak at 88 aa indicates the unfolding of helix E, that at 94 of loop DE, and the peak at 105 corresponds to the unfolding of helix D. The shoulder peaks of the second major peak at 148 aa indicate the stepwise unfolding of helices C and B and loop BC. The peak at 148 aa indicates the unfolding of helix C, that at 158 of loop BC, and the peak at 175 aa represents unfolding of helix B. The unfolding scheme *via* the different pathways is shown at the bottom. The arrows indicate the observed unfolding pathways. In certain pathways (black arrows), a pair of transmembrane helices and their connecting loop unfolded in a single step. In other unfolding pathways (colored arrows), these structural elements unfolded in several intermediate steps. The color code of the force–extension curves corresponds to that of the arrows in the pathways shown below. It should be noted that more than 360 unfolding curves were analyzed in this work. Each unfolding barrier occurred at certain probabilities in an unfolding curve.[28–30,35] Thus, within given probabilities, average forces and contour lengths of unfolded polypeptides (Figures 4–6 and Table 1), an individual unfolding curve can show deviations from the one represented here. In most cases, differences between two randomly selected unfolding curves will be within a few minor peaks. Classification of each unfolding curve shows at which probability the corresponding unfolding pathway occurred.

structures of the protein can unfold either in a collective process such as that observed by the pairwise unfolding of transmembrane α-helices (see above) or in a stepwise manner. The similarity of the unfolding pathways observed for single BR molecules being assembled into trimers and dimers, and monomers is shown in Figure 4.

Unfolding of single BR molecules from different assemblies occurs at different forces

Figure 5 shows the magnitude of unfolding forces of each main and each side peak observed for BR monomeric, dimeric and trimeric forms. The most noticeable change in unfolding force for all three BR forms was observed for the grouped unfolding of helices E and D (Figure 5(a), Table 1). For unfolding a single BR molecule out of a trimer, the unfolding force of the helical pair E and D (151(±29) pN, average (±SD), $n=39$), was larger than that for helices B and C (107(±37) pN, $n=51$), and for the unfolding of helix A including the N terminus (90(±20) pN, $n=103$). A similar trend was observed for unfolding a BR molecule from the BR dimer. The unfolding force of paired helices E and D (140(±29) pN, $n=74$) was higher than that for helices B and C (95(±30) pN, $n=66$) and for helix A (96(±22) pN, $n=171$). The pattern was observed again for unfolding of the BR monomer. Forces to unfold the helical pair E and D (98(±34) pN, $n=43$) were above those required to unfold helices B and C (82(±29) pN, $n=54$) and helix A (including the N terminus) (78(±24) pN, $n=65$).

The average unfolding forces (Figure 5(a), Table 1) suggested that the force for unfolding of the paired helices E and D was the highest for the BR trimer (151(±29) pN), decreased for the dimer (140(±29) pN), and was the least for the monomer (98(±34) pN). Similarly, the force for unfolding of helices B and C in a pairwise manner dropped from trimer (107(±37) pN) to monomer (82(±29) pN) BR assembly. In agreement with the above observations the grouped unfolding force of helix A and its N-terminal end was higher for the trimeric assembly (90(±20) pN) than for the monomer (78(±24) pN). As observed previously,[28] the rupture forces of helical pairs decreased with the number of structural elements that have been unfolded before. Figure 5(b) (Table 1) shows the magnitude of unfolding forces of each side peak for all BR types. As indicated, the unfolding forces for individual secondary structure elements in the BR assemblies investigated were approximately the same (Figure 5(b), Table 1).

Probability to choose a given unfolding pathway depends on BR assembly

As reported previously, BR molecules in the trimeric assembly followed well-defined unfolding pathways and the unfolding of transmembrane helices occurred predominantly in a pairwise fashion.[27,28,30,35] Here, we scrutinized the unfolding

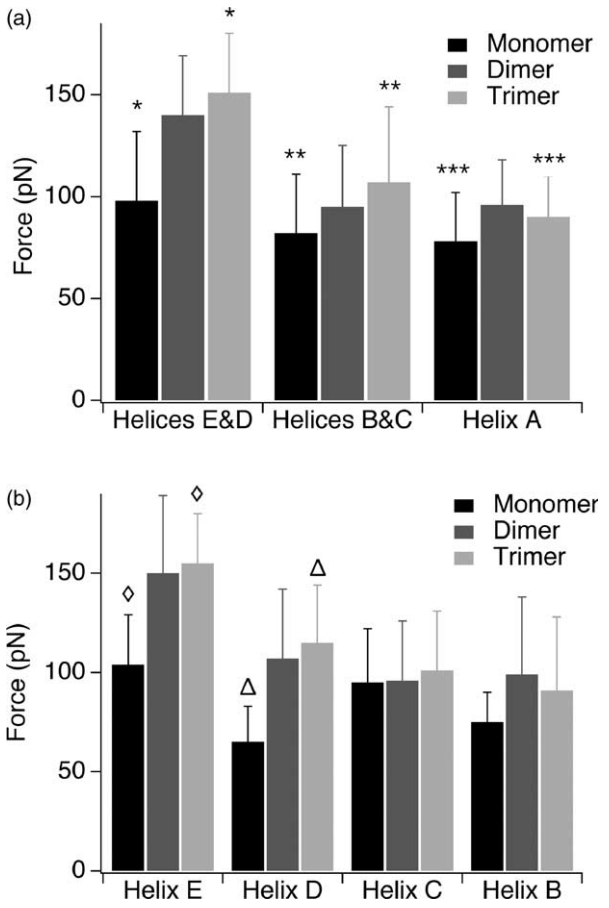

Figure 5. Unfolding forces of secondary structure elements in trimeric, dimeric and monomeric BR. (a) Rupture forces of main peaks that exhibited no side peaks. The forces represent the pairwise unfolding of transmembrane α-helices E and D (88 aa), B and C (148 aa), and the unfolding of helix A (219 aa). The main peak representing the pairwise unfolding of helices G and F is not shown because unspecific surface interactions between the AFM stylus and the PM scatter the position and the appearance of the force peaks significantly. Unfolding forces for each pair of helices, E and D, and B and C, and single helix A (with the N terminus), increase from monomer to trimer, suggesting that the mechanical stability of trimeric assembly is higher than monomeric assembly; (*) $p<0.0001$, (**) $p=0.0003$, (***) $p=0.01$ (one-way ANOVA followed by Bonferroni's post-test). For helices E and D, $p<0.0001$ comparing monomer with dimer and trimer, respectively, and $p=0.2$ on dimer–trimer comparison. For helices B and C, $p=0.0003$ on monomer with trimer comparison, $p=0.1$ on comparing dimer with trimer and monomer, respectively. For helix A, $p=0.01$ for trimer–monomer, $p=0.08$ for dimer–trimer, and $p<0.0001$ for dimer–monomer comparisons. (b) Unfolding forces of side peaks represent unfolding of single α-helices and connecting loops. Except for single helices E and D, the unfolding forces for single helices are similar for all the three types of BR. (◊) $p<0.0001$; (△) $p=0.0032$. Error bars are the standard deviations. The number of single-molecule unfolding spectra analyzed were $n=77$ (monomer), $n=176$ (dimer) and $n=124$ (trimer).

Table 1. Unfolding force, contour length and probability of occurrence of secondary structure elements and structural segments unfolding in a pairwise or stepwise manner

	Average unfolding force ± SD (pN)			Occurrence ± error (%)			Average contour length ± SD (aa)		
Helices unfolded	Trimer	Dimer	Monomer	Trimer	Dimer	Monomer	Trimer	Dimer	Monomer
E◇	155 ± 25	150 ± 39	104 ± 25	33.1 ± 4.2	22.2 ± 3.1	22.1 ± 4.7	105.9 ± 9.2	108.2 ± 9.7	105.3 ± 4.6
D△	115 ± 29	107 ± 35	65 ± 18	50.8 ± 4.5	40.4 ± 3.7	30 ± 5.2	145.8 ± 4	144 ± 4.9	145.6 ± 5.4
E&D*	151 ± 29	140 ± 29	98 ± 34	31.5 ± 4.2	42 ± 3.7	55.8 ± 5.7	–	–	–
C	101 ± 30	96 ± 30	95 ± 27	36.3 ± 4.3	33.7 ± 3.5	15.6 ± 4.1	159.3 ± 1.5	152.1 ± 2.5	158.9 ± 2.8
B	91 ± 37	99 ± 39	75 ± 15	31.5 ± 4.2	39 ± 3.7	19.5 ± 4.5	216.3 ± 7.1	210.7 ± 5.7	217 ± 6.5
B&C**	107 ± 37	95 ± 30	82 ± 29	41 ± 4.4	37.5 ± 3.6	70.1 ± 5.2	–	–	–
C&loop BC	99 ± 30	98 ± 28	93 ± 34	22.6 ± 3.7	29 ± 3.4	14.3 ± 4	169.6 ± 4.3	164 ± 4.2	172.9 ± 2.9
Loop BC & B	100 ± 50	120 ± 56	103 ± 33	27.4 ± 4	24 ± 3.2	10.4 ± 3.5	216.3 ± 7.1	210.7 ± 5.7	217 ± 6.5
Loop BC	117 ± 35	94 ± 29	85 ± 17	8.9 ± 2.5	9.7 ± 2.2	5.2 ± 2.5	–	–	–
A (N-terminal)***	90 ± 20	96 ± 22	78 ± 24	83 ± 3.4	97.2 ± 1.2	84.4 ± 4.1	Molecule extracted from the membrane (248 aa)		

Within the same BR form (trimer, dimer and monomer), forces for pairwise unfolding of helices E and D are higher than for pairwise unfolding of helices B and C, and helix A (and N-terminal) (for BR trimer, $p < 0.0001$ on comparing unfolding of helices E and D with helices B and C, and helix A respectively, $p = 0.0005$ comparing helices B and C with helix A; for BR dimer, $p < 0.0001$ comparing helices E and D with helices B and C, and helix A respectively, $p = 1$ for helices B and C with helix A comparison; for BR monomer, $p = 0.02$ on comparing helices E and D with helices B and C, $p = 0.003$ comparing helices E and D with helix A, $p = 1$ comparing helices B and C with helix A). (*), (**), (◇) and (△) denote the same as given in the legend to Figure 5. In all, 77 force extension curves were analyzed for the BR monomer, 176 for the BR dimer and 124 for the BR trimer.

pathways of BR in different forms and observed that these unfolding pathways do not change upon formation of BR monomers, dimers or trimers (Figure 4).

In contrast to the unfolding pathways, their probability of occurrence depended on the BR assemblies. For all three BR forms the probability of transmembrane helices to unfold in a pairwise manner (Figure 6) was highest for monomeric BR. For pairwise unfolding of helices E and D, and helices B and C, the probability increased from trimer to monomer. The probability for unfolding of helical pair E and D was 31(±4)% (average ± absolute error, $n = 39$) for trimeric BR, 42(±4)% ($n = 74$) for dimeric BR and 56(±6)% ($n = 43$) for monomeric BR. In the same order, the probability for pairwise unfolding of helices B and C increased from BR trimer 41(±4)% ($n = 51$) to BR monomer 70(±5)% ($n = 54$).

Discussion

Unfolding pathways remain the same but their probability depends on BR assembly

All BR assemblies investigated showed similar subsets of force extension curves recorded upon unfolding single molecules (Figures 3 and 4). This indicates that the BR molecules could choose among identical unfolding pathways. However, the probability of a BR molecule to choose one individual unfolding pathway from the various unfolding pathways strongly depended on its assembly. For example, the probability distribution shows that the rate for pairwise unfolding of transmembrane helices was higher for monomeric BR than that for BR assembled into dimers and trimers (Figure 6). We conclude that oligomerization of BR supports unfolding of structural segments individually, while unfolding in the BR monomer occurs predominantly in a pairwise fashion. A similar trend was observed on unfolding single BR molecules from the trimeric assembly at temperatures ranging from 8 °C to 52 °C.[35] While at low temperatures the single helices and loops exhibited an enhanced probability to unfold in single events, their probability to unfold groupwise increased with temperature. Considering that temperature serves as a denaturant[36,37] we assume that in both cases the reduction of mechanical stability supports pathways with groupwise unfolding of structural segments.

Furthermore, our results strongly suggest that unfolding pathways of BR depend on whether the

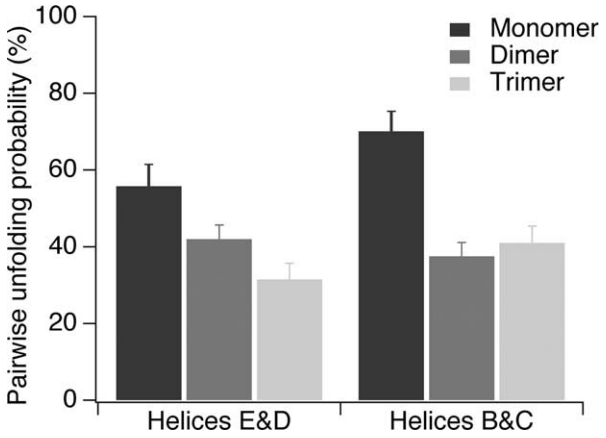

Figure 6. Probability of pairwise unfolding pathways. Probability of pairwise unfolding of helices increased from trimer to monomer. Error bars show the absolute errors calculated using the formula $\sqrt{p(1-p)/n}$, where p is the unfolding probability *via* a certain pathway, n is the number of molecules unfolded. The number of unfolding curves analyzed were $n = 77$ (monomer), $n = 176$ (dimer) and $n = 124$ (trimer).

membrane proteins were unfolded from their trimer, dimeric or monomeric form. Considering that not only the oligomeric state but also the lipid environment of the BR establishes the overall system, which guides the membrane protein to populate certain unfolding pathways, important conclusions may be drawn for unfolding experiments in general. In most unfolding experiments of membrane proteins the protein is removed from the membrane by detergent.[38] Albeit, being functional in detergent it can be conveniently assumed here that the altered environment of the membrane protein may change the population of certain unfolding pathways in these experiments. The same can be concluded if the oligomeric state of the solubilized membrane protein unfolded is not the native one. Similarly, it was recently observed that small temperature changes in the environment guide single BR molecules to unfold *via* different unfolding pathways being populated by different unfolding intermediates as indicated by their occurrence probability.[35] Thus, to prevent the characterization of unfolding pathways that a membrane protein would not necessarily take *in vivo*, with mechanical, chemical or thermal unfolding experiments, unfolding experiments should be performed in the native or at least in the native-like environment of the membrane protein.

Location of stable structural segments is independent of BR assembly

Force extension curves recorded upon unfolding of BR from monomers, dimers and trimers exhibited force peaks at identical positions (Figures 3 and 4). This suggests that a change in the oligomeric state and of the lateral assembly of the BR oligomers within the membrane does not influence the position of the unfolding barriers. Thus, it can be concluded that in our measurements intermolecular interactions occurring between proteins or between proteins and lipids did not change the location of structural segments that stabilize the protein and establish the unfolding barriers. Considering that the tertiary structure of BR did not change significantly upon oligomerization,[21,37] it may be concluded that the stable segments and the secondary structures may be somehow related.[30] Currently it is difficult to understand how they are linked to each other, since some of the stable structural segments can bridge two or more secondary structures, while in some cases they stabilize only one-third of a helix.[28,30]

Membrane protein assembly changes stability of structural segments

Unfolding of BR from the trimeric form occurred at higher forces compared to the dimeric and monomeric BR forms, as suggested by the forces required to unfold paired or single secondary structure elements (Table 1). Overall, the results allow us to conclude that BR assembled in a trimeric arrangement is mechanically more stable than BR in the dimeric or monomeric forms. In apparent contrast, the size and location of structural segments establishing the unfolding barriers within the membrane are the same as those observed for the native trimeric assembly. Thus, we suggest that BR molecules do not establish new unfolding barriers in their monomeric or dimeric forms but that interactions establishing these barriers are strengthened by the increasing complexity of the assembly.

Changing the membrane protein assembly of BR is associated with changing the lipids directly attached to the protein. Thus, BR molecule and lipid environment mainly determine whether the BR forms a monomer, dimer or trimer. When investigating why the oligomeric state of the BR influences the unfolding barriers, possible contributions of lipids should be considered. Structural investigations suggest that lipid molecules stabilize BR trimers by specific interactions of their head group moieties.[16,17] Therefore, this topic should be discussed in further detail. Since the exact lipid environment and arrangement of the BR assemblies investigated here are not resolved yet, we exclude these considerations.

Revealing contributions of inter- and intramolecular interactions

Forces required to unfold individual secondary structure elements are shown in Table 1. These unfolding steps are represented by the main and side peaks in the force–extension spectra (Figure 4). Except for individual helices E and D, for which the unfolding force decreased significantly from trimer to monomer, unfolding of the corresponding individual secondary structure elements occurred at slightly decreasing forces (Figure 5(b)). It is intriguing that, in spite of the differences in BR assemblies, almost the same forces are required to unfold helices C, B and A individually. We attribute this similarity as arising from unchanged intramolecular interactions that may dominate these secondary structure elements against destabilizing or stabilizing factors from the environment. This leads to an important conclusion. Dimeric or monomeric BRs have clearly different structural constraints, which to some extent can limit the conformational freedom of certain secondary structures during unfolding. However, the similar forces required to unfold individual helices suggest that the intrinsic stability of these structures may be the same but that their unwinding may be easier on comparing one assembly with the other.

The analyses of the experimental data allow insights into the complex contributions of inter- and intramolecular interactions to the overall stability of a structural segment. Stable structural segments established in monomeric BR are mostly the result of intramolecular interactions. Oligomerization can contribute significantly to their

stability. Simple subtraction allows us to determine the contribution of intermolecular interactions that enhance the mechanical stability of structural segments that stabilize secondary structure elements. For example, trimerization of BR contributes ~50 pN to the stability of helix E and ~25 pN to loop BC. Division of the absolute unfolding force values from two oligomeric assemblies allows calculation of the percentage of increasing stability due to intermolecular interactions.

Recently, advanced DFS experiments allowed the determination of conservative and dissipative contributions during unfolding single structural segments of BR.[39] Such and other insights revealed by advanced analysis methods[40] may in future enable us to draw even more detailed pictures of the unfolding process. However, it may be speculated that even more sensitive force detection approaches using small cantilevers may allow the unraveling of the breakage of single hydrogen or ionic bonds initiating the unfolding process. Taking a closer look at some of the force-spectra sometimes reveals small force modulations, which could indicate such a behavior. However, at this moment such assumptions are too speculative to be made on a scientifically solid basis.

Relation to chemical and thermal denaturation experiments

Conventionally, unfolding of BR is studied by chemical or thermal denaturation. Such experiments have shown that lipids,[23,41] detergents[21,42] and electrolytes,[23,43] could have strong influences on BR assembly, stability and function. It was also shown that monomeric BR unfolds at lower temperatures compared to trimeric BR. The denaturational transition at ~100 °C of BR trimer as measured by differential scanning calorimetry exhibited an enthalpy change of 100 kcal/mol.[36,44,45] Monomeric BR in detergent is denatured with a nearly identical enthalpy change (95 kcal/mol), although at a lower temperature of 80 °C.[37] This suggests that trimeric BR is marginally more stable and has a higher activation energy of transition as compared to monomeric BR. The possible reasons for this behavior could be trimer formation of BR and hence more favorable energetics of association between trimers in the lattice. Pairwise unfolding forces of helices E and D, and helices B and C are higher for BR trimer than for dimer and monomer. The probability for pairwise unfolding of these helices, on the other hand, is lowest for BR assembled into a trimer. Though a comparison of conventional (bulk measurements) and forced unfolding experiments is not relevant, it can be suggested on the basis of these data that the greater stability of trimeric and dimeric BR as compared to monomeric BR is due to stronger monomer–monomer and monomer–lipid interactions leading to higher intrinsic stability of the two systems.

Functional implications

As suggested by the lower unfolding force and higher probability, the unfolding pathway of a monomer existing independently in the membrane is energetically and kinetically more favorable than in a trimeric assembly. Stabilization of monomers is hence achieved by trimer formation and arrangement into a crystal lattice structure for its efficient function as a proton pump. The long life-cycle of this molecule is a guarantee for photosynthetic growth in nature over a period of months under intense sunshine without photochemical destabilization. Nevertheless, our unfolding data suggest that the BR monomer is a structurally stable biological unit, which also occurs in some halobacterial species as the functional unit.[46] Thus it seems that in *H. salinarum* the lattice formation of the purple membrane serves a functional stabilization, whereas in other strains intramolecular forces may provide this stabilization. It will be interesting to test this hypothesis by force spectroscopy experiments with the Mexican or Australian halobacterial strains mex, port or shark.[46]

Experimental Procedures

Purple membrane preparation, dimerization and monomerization of BR

Wild-type purple membrane (PM) was extracted from *H. salinarum* and purified as described.[47] Dimerization of BR with DTAC (*n*-dodecyl trimethylammonium chloride) was carried out following the procedure described by Michel *et al*.[21] Monomeric BR was formed in the cell membrane of *H. salinarum* after introducing point mutations at positions 12 and 80 (W12/80I).[22] The respective tryptophan residues were substituted by isoleucine residues. Cells were lyzed and membranes fractionated on sucrose density gradients. As no purple membranes were formed in the mutant strains, the fractions containing the highest BR content were used for the AFM experiments. The mutations introduced only disrupted trimer–trimer interactions (W12I) and monomer–monomer interactions (W80I) within the trimer, and did not alter the structure–function relationship of BR, which was characterized by the unchanged photocycle. All buffer solutions were prepared using nanopure water (18 MΩ/cm) and p.a. grade chemicals from Sigma/Merck.

Attachment of BR to the AFM cantilever

BR was attached non-specifically to silicon nitride cantilever by applying a contact force of ~1 nN between the AFM stylus and the membrane surface. This method has been shown to provide equivalent results and allows a much higher throughput as compared to specific attachment *via* thiol–gold linkage.[27]

Single-molecule force spectroscopy and imaging

Single-molecule AFM imaging and force spectroscopy was performed as described earlier.[27,28] A few microlitres

of the membrane sample was adsorbed onto freshly cleaved mica surface in 300 mM KCl, 20 mM Tris (pH 7.8). To determine the BR assembly, membrane patches were imaged at high resolution using contact mode AFM.[32,33] For force measurements, the AFM stylus was approached to the membrane protein surface while applying a constant force of <1 nN. After a contact time of ~ 1 s, the stylus was retracted from the membrane surface at a constant velocity of 300 nm/s. In about 10% (trimeric BR), $\sim 5\%$ (dimeric BR) and $\sim 2\%$ (monomeric BR) of cases we detected one or more adhesion peaks. All experiments were performed in 300 mM KCl, 20 mM Tris–HCl (pH 7.8), at room temperature (24($\pm$1) °C).

Spring constants of the 200 μm long silicon nitride AFM cantilevers (NPS, Veeco Metrology; nominal spring constant ~ 0.08 N/m) were calibrated in buffer solution using the equipartition theorem.[48,49] All cantilevers used were from the same cantilever batch and exhibited similar spring constants within the uncertainty of this method ($\sim 10\%$). To rule out statistical errors due to cantilever spring constant deviations, the force spectroscopy experiments were performed on each BR assembly using at least five different cantilevers from the same batch. Additionally, we used a single cantilever to record 20 force extension curves on each of the BR assemblies. These test experiments did not show significant deviations from the experimental results when using taking different cantilevers to reveal higher statistics.

Selection and analysis of force–extension curves

We have previously identified force–extension curves that result from mechanical unfolding of single BR molecules from their C-terminal end. Force extension curves exhibiting an overall length between 60 nm and 70 nm reflect completely unfolded and extended BR molecules attached by their C-terminal end to the AFM stylus.[27,28] All force–extension curves exhibiting these overall unfolding spectra and lengths were selected and aligned using identical procedures and criteria established previously.[28] Every peak of a single force–extension curve was fitted using the worm-like chain model (WLC) with a persistence length of 0.4 nm and a monomer length of 0.36 nm.[25] The number of extended amino acids at each peak was then calculated using the contour length obtained from the WLC fits. This allowed us to assign unfolding events to structural segments of BR such as described before.[28] The structural BR model described by Mitsuoka *et al.* (PDB 1AT9)[19] was chosen. To measure the unfolding force and probability of unfolding for each individual structural segment, every event of each curve was analyzed. To determine if the average forces represent the true means of the given population and are statistically different, the data were tested against one-way ANOVA analysis followed by Bonferroni's post-test. The p value obtained from this is the probability (from 0 to 1) of observing a difference as large or larger than one would observe if the null hypothesis is true.

Acknowledgements

We thank H. Janovjak, A. Kedrov, D. Cisneros, J. Lakey and P.-H. Puech for stimulating discussions. The Volkswagenstiftung, free state of Saxony, and European Union supported this work.

References

1. Engelman, D. & Steitz, T. (1981). The spontaneous insertion of proteins into and across membranes: the helical hairpin hypothesis. *Cell*, **23**, 411–422.
2. White, S. & Wimley, W. (1999). Membrane protein folding and stability: physical principles. *Annu. Rev. Biophys. Biomol. Struct.* **28**, 319–365.
3. White, S. (2003). Translocons, thermodynamics, and the folding of membrane proteins. *FEBS Letters*, **555**, 116–121.
4. Engelman, D., Chen, Y., Chin, C., Curran, A., Dixon, A., Dupuy, A. *et al.* (2003). Membrane protein folding: beyond the two stage model. *FEBS Letters*, **555**, 122–125.
5. Haltia, T. & Freire, F. (1995). Forces and factors that contribute to the structural stability of membrane proteins. *Biochim. Biophys. Acta*, **1228**, 1–27.
6. Prusiner, S. (1997). Prion diseases and the BSE crisis. *Science*, **278**, 245–251.
7. Martin, J. (1999). Molecular basis of the neurodegenerative disorders. *N. Engl. J. Med.* **340**, 1970–1980.
8. Dobson, C. (2002). Getting out of shape. *Nature*, **418**, 729–730.
9. Oesterhelt, D. & Stoeckenius, W. (1971). Rhodopsin-like protein from the purple membrane of *Halobacterium halobium*. *Nature New Biol.* **233**, 149–152.
10. Haupts, U., Tittor, J. & Oesterhelt, D. (1999). Closing in on bacteriorhodopsin: progress in understanding the molecule. *Annu. Rev. Biophys. Biomol. Struct.* **28**, 367–399.
11. Subramaniam, S., Gerstein, M., Oesterhelt, D. & Henderson, R. (1993). Electron diffraction analysis of structural changes in the photocycle of bacteriorhodopsin. *EMBO J.* **12**, 1–8.
12. Lanyi, J. K. (2004). Bacteriorhodopsin. *Annu. Rev. Physiol.* **66**, 665–688.
13. Hargrave, P. (1991). Seven-helix receptors. *Curr. Opin. Struct. Biol.* **1**, 575–581.
14. Baldwin, J. (1993). The probable arrangement of the helices in G protein-coupled receptors. *EMBO J.* **12**, 1693–1703.
15. Filipek, S., Teller, D. C., Palczewski, K. & Stenkamp, R. (2003). The crystallographic model of rhodopsin and its use in studies of other G protein-coupled receptors. *Annu. Rev. Biophys. Biomol. Struct.* **32**, 375–397.
16. Essen, L., Siegert, R., Lehmann, W. & Oesterhelt, D. (1998). Lipid patches in membrane protein oligomers: crystal structure of the bacteriorhodopsin–lipid complex. *Proc. Natl Acad. Sci. USA*, **95**, 11673–11678.
17. Grigorieff, N., Ceska, T., Downing, K., Baldwin, J. & Henderson, R. (1996). Electron-crystallographic refinement of the structure of bacteriorhodopsin. *J. Mol. Biol.* **259**, 393–421.
18. Luecke, H., Schobert, B., Richter, H., Cartailler, J. & Lanyi, J. (1999). Structure of bacteriorhodopsin at 1.55 Å resolution. *J. Mol. Biol.* **291**, 899–911.
19. Mitsuoka, K., Hirai, T., Murata, K., Miyazawa, A., Kidera, A., Kimura, Y. & Fujiyoshi, Y. (1999). The structure of bacteriorhodopsin at 3.0 Å resolution based on electron crystallography: implication of the charge distribution. *J. Mol. Biol.* **286**, 861–882.

20. Blaurock, A. & Stoeckenius, W. (1971). Structure of the purple membrane. *Nature New Biol.* **233**, 152–155.
21. Michel, H., Oesterhelt, D. & Henderson, R. (1980). Orthorhombic two-dimensional crystal form of purple membrane. *Proc. Natl Acad. Sci. USA*, **77**, 338–342.
22. Weik, M., Patzelt, H., Zaccai, G. & Oesterhelt, D. (1998). Localization of glycolipids in membranes by *in vivo* labeling and neutron diffraction. *Mol. Cell*, **1**, 411–419.
23. Mukhopadhyay, A., Dracheva, S., Bose, S. & Hendler, R. (1996). Control of the integral membrane protein pump, bacteriorhodopsin, by purple membrane lipids of *Halobacterium halobium*. *Biochemistry*, **35**, 9245–9252.
24. Heyes, C. & El-Sayed, M. (2002). The role of the native lipids and lattice structure in bacteriorhodopsin protein conformation and stability as studies by temperature-dependent Fourier transform-infrared spectroscopy. *J. Biol. Chem.* **277**, 29437–29443.
25. Rief, M., Gautel, M., Oesterhelt, F., Fernandez, J. & Gaub, H. (1997). Reversible unfolding of individual titin immunoglobulin domains by AFM. *Science*, **276**, 1109–1112.
26. Carrion-Vazquez, M., Oberhauser, A. F., Fowler, S. B., Marszalek, P. E., Broedel, S. E., Clarke, J. & Fernandez, J. M. (1999). Mechanical and chemical unfolding of a single protein: a comparison. *Proc. Natl Acad. Sci. USA*, **96**, 3694–3699.
27. Oesterhelt, F., Oesterhelt, D., Pfeiffer, M., Engel, A., Gaub, H. & Müller, D. J. (2000). Unfolding pathways of individual bacteriorhodopsins. *Science*, **288**, 143–146.
28. Müller, D., Kessler, M., Oesterhelt, F., Moeller, C., Oesterhelt, D. & Gaub, H. (2002). Stability of bacteriorhodopsin a-helices and loops analyzed by single-molecule force spectroscopy. *Biophys. J.* **83**, 3578–3588.
29. Janovjak, H., Struckmeier, J., Hubain, M., Kedrov, A., Kessler, M. & Müller, D. J. (2004). Probing the energy landscape of the membrane protein bacteriorhodopsin. *Structure*, **12**, 871–879.
30. Cisneros, D., Oesterhelt, D. & Müller, D. J. (2005). Probing origins of molecular interactions stabilizing the membrane proteins halorhodopsin and bacteriorhodopsin. *Structure*, **13**, 235–242.
31. Müller, D. J. & Engel, A. (1997). The height of biomolecules measured with the atomic force microscope depends on electrostatic interactions. *Biophys. J.* **73**, 543–549.
32. Müller, D. J., Sass, H., Müller, S., Büldt, G. & Engel, A. (1999). Surface structures of native bacteriorhodopsin depend on the molecular packing arrangement in the membrane. *J. Mol. Biol.* **285**, 1903–1909.
33. Moeller, C., Büldt, G., Dencher, N., Engel, A. & Müller, D. J. (2000). Reversible loss of crystallinity on photobleaching purple membrane in the presence of hydroxylamine. *J. Mol. Biol.* **301**, 869–879.
34. Müller, D. J., Engel, A., Matthey, U., Meier, T., Dimroth, P. & Suda, K. (2003). Observing membrane protein diffusion at subnanometer resolution. *J. Mol. Biol.* **327**, 925–930.
35. Janovjak, H., Kessler, M., Oesterhelt, D., Gaub, H. & Müller, D. J. (2003). Unfolding pathways of native bacteriorhodopsin depend on temperature. *EMBO J.* **22**, 5220–5229.
36. Jackson, M. & Sturtevant, J. (1978). Phase transitions of the purple membranes of *Halobacterium halobium*. *Biochemistry*, **17**, 911–915.
37. Brouillette, C., McMichens, R., Stern, L. & Khorana, H. (1989). Structure and thermal stability of monomeric bacteriorhodopsin in mixed phospholipid/detergent micelles. *Proteins: Struct. Funct. Genet.* **5**, 38–46.
38. Booth, P. J., Templer, R. H., Meijberg, W., Allen, S. J., Curran, A. R. & Lorch, M. (2001). *In vitro* studies of membrane protein folding. *Crit. Rev. Biochem. Mol. Biol.* **36**, 501–603.
39. Janovjak, H., Muller, D. J. & Humphris, A. D. L. (2005). Molecular force modulation spectroscopy revealing the dynamic response of single bacteriorhodopsins. *Biophys. J.* **88**, 1423–1431.
40. Janovjak, H., Sapra, T. & Muller, D. J. (2005). Complex stability of single proteins explored by forced unfolding experiments. *Biophys. J.* **88**, L37–L39.
41. Dracheva, S., Bose, S. & Hendler, R. (1996). Chemical and functional studies on the importance of purple membrane lipids in bacteriorhodopsin photocycle behavior. *FEBS Letters*, **382**, 209–212.
42. Huang, K., Bayley, H. & Khorana, H. (1980). Delipidation of bacteriorhodopsin and reconstitution with exogenous phospholipids. *Proc. Natl Acad. Sci. USA*, **77**, 323–327.
43. Sternberg, B., L'Hostis, C., Whiteway, C. & Watts, A. (1992). The essential role of specific *Halobacterium halobium* polar lipids in 2D-array formation of bacteriorhodopsin. *Biochim. Biophys. Acta*, **1108**, 21–30.
44. Kahn, T., Sturtevant, J. & Engelman, D. (1992). Thermodynamic measurements of the contributions of helix-connecting loops and of retinal to the stability of bacteriorhodopsin. *Biochemistry*, **31**, 8829–8839.
45. Brouillette, C., Muccio, D. & Finney, T. (1987). pH dependence of bacteriorhodopsin thermal unfolding. *Biochemistry*, **26**, 7431–7438.
46. Otomo, J., Tomioka, H. & Sasabe, H. (1992). Bacterial rhodopsins of newly isolated halobacteria. *J. Gen. Microbiol.* **138**, 1027–1037.
47. Oesterhelt, D. & Stoeckenius, W. (1974). Isolation of the cell membrane of *Halobacterium halobium* and it fraction into red and purple membrane. *Methods Enzymol.* **31**, 667–678.
48. Florin, E., Rief, M., Lehmann, H., Ludwig, M., Dornmair, C., Moy, V. & Gaub, H. (1995). Sensing specific molecular interactions with the atomic force microscope. *Biosense. Bioelectron.* **10**, 895–901.
49. Butt, H. & Jaschke, M. (1995). Calculation of thermal noise in atomic force microscopy. *Nanotechnology*, **6**, 1–7.

Edited by W. Baumeister

(Received 3 August 2005; received in revised form 19 October 2005; accepted 28 October 2005)
Available online 17 November 2005